



<https://doi.org/10.36023/ujrs.2023.10.1.231>

UDC 004.932

## Analysis of the potential efficiency of post-filtering noisy images after lossy compression

B. V. Kovalenko\*, V. S. Rebrov, V. V. Lukin

Department of Information and Communication Technologies named after O.O. Zelensky, National Aerospace University, 61070 Kharkiv, Ukraine

An increase in the number of images and their average size is the general trend nowadays. This increase leads to certain problems with data storage and transfer via communication lines. A common way to solve this problem is to apply lossy compression that provides sufficiently larger compression ratios compared to lossless compression approaches. However, lossy compression has several peculiarities, especially if a compressed image is corrupted by quite intensive noise. First, a specific noise-filtering effect is observed. Second, an optimal operational point (OOP) might exist where the quality of a compressed image is closer to the corresponding noise-free image than the quality of the original image according to a chosen quality metric. In this case, it is worth compressing this image in the OOP or its closest neighborhood. These peculiarities have been earlier studied and their positive impact on image quality improvement has been demonstrated. Filtering of noisy images due to lossy compression is not perfect. Because of this, it is worth checking can additional quality improvement be reached using such an approach as post-filtering. In this study, we attempt to answer the questions: “is it worth to post-filter an image after lossy compression, especially in OOP’s neighborhood? And what benefit can it bring in the sense of image quality?”. The study is carried out for better portable graphics (BPG) coder and the DCT-based filter focusing mainly on one-component (grayscale) images. The quality of images is characterized by several metrics such as PSNR, PSNR-HVS-M, and FSIM. Possible image quality increasing via post-filtering is demonstrated and the recommendations for filter parameter setting are given.

**Keywords:** grayscale images, lossy image compression, optimal operation point, BPG coder, post-filtering, DCT-based filter

© B. V. Kovalenko, V. S. Rebrov, V. V. Lukin. 2023

### 1. Introduction

The technology of sensors’ design and manufacturing has been rapidly developing in recent years (Mehmood et al., 2022 and Bazi et al., 2022). That has led not only to the better spatial resolution of images but also considerable size increase of acquired images (Ma et al., 2015). In addition, it has become popular to get multiple images of the same terrain, which has resulted in even greater problems in the transmission and storage of information data (Schowengerdt et al., 2007 and Blanes et al., 2014). A common way to solve this problem is to apply some image compression techniques.

In general, the use of lossless and lossy compression approaches is possible (Hussain et al., 2018). An advantage of lossless compression is that it introduces no distortions into data. However, the compression ratio (CR) attained by lossless compression techniques is often too small (not appropriate for many applications), especially for images corrupted by noise. Lossy compression allows for reaching larger and variable CR values. Meanwhile, a larger CR results in larger distortions introduced (Ponomarenko et al., 2005). Then, a reasonable trade-off has to be found and provided (Christophe et al., 2011).

It is worth stressing that compression should not be only intended on reaching this trade-off, but it also has to take into account the peculiarities of images and possible noise presence (Penna et al., 2007 and Kovalenko et al., 2021). This is due to the fact that, in practice, it is hard to find images without noise (although this noise can be invisible for low intensities), especially in remote sensing (RS) images that are often corrupted by a rather intensive noise.

In the case one wants to provide a high quality of lossy compressed noisy images with a simultaneous desire to have a sufficiently high CR, compression in the so-called optimal operation point (OOP) can be a prominent solution. OOP is such a parameter of a coder that provides the minimal difference (according to some quality metric) between the compressed and noise-free image. Previously, we have demonstrated the benefits of using the OOP parameter in the lossy compression of noisy images. In many cases, it worked well and showed good results in terms of improving image quality (Kovalenko et al., 2022).

For some applications, it is necessary to provide even better quality. Then, such an approach as compressed image post-filtering can be applied (Simmer et al., 2001). By post-filtering, we mean that some denoising technique (in our case, it is the DCT-based filter) is applied after the compression of a noisy image in the OOP neighborhood. Although lossy compression of the

\*E-mail: [b.kovalenko@khai.edu](mailto:b.kovalenko@khai.edu)

noisy image in this case already provides quality improvement (if OOP exists), it is reasonable to check can the post-filtering with properly adjusted parameters further improve the quality and how large that improvement can be. A side task is also the optimal or quasi-optimal setting of the post-filter parameters.

This paper concentrates on post-filtering by the DCT-based filter (Ponomarenko et al., 2011) of noisy grayscale images after lossy compression by BPG (better portable graphics) coder (Bellard et al., 2018). To estimate the improvement in image quality, such quantitative criteria as peak signal-to-noise ratio (PSNR) and visual quality metrics PSNR–HVS–M (Ponomarenko et al., 2007) and FSIM (Zhang et al., 2011) are employed.

## 2. Experiment setup

### 2.1. Image/noise properties and the used metrics

As test images, two typical representatives of remote sensing data have been taken – these are images Frisco and fr03 presented in Fig. 1. The first image is an example of simple structure images whilst the second one relates to middle complexity images. As has been mentioned in Introduction, in practice it is difficult to acquire noise-free images, especially RS ones. Noise can appear in images due to many factors; it can be visible or invisible (Chatterjee et al., 2010). Visible noise has an essential impact on image visual quality and classification accuracy. That is why, we concentrate here on the case of visible noise typical, e.g., for images acquired in bad illumination conditions.

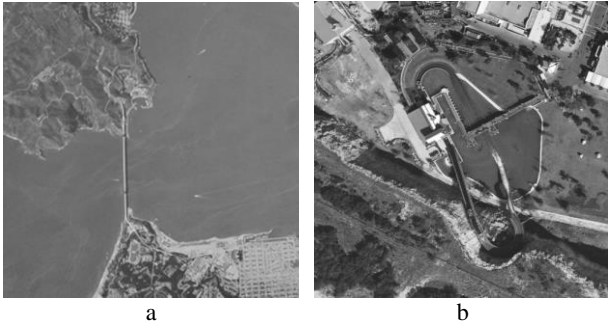


**Fig. 1.** Used test images Frisco (a), fr03 (b)

In this work, we consider additive white Gaussian noise (AWGN), which is known to be the simplest noise model and can be a good starting point in research. According to this model, one has

$$I_{ij}^n = I_{ij}^{true} + n_{ij}, \quad (1)$$

where  $I_{ij}^n$  denotes the noisy  $ij$ -th pixel value,  $I_{ij}^{true}$  is the true  $ij$ -th pixel value,  $n_{ij}$  is the value of AWGN having zero mean and variance  $\sigma^2$ . Below we assume that noise variance is already known or accurately pre-estimated (Colom et al., 2014 and Selva et al., 2021).

To estimate the quality of noisy or processed images, one can use various metrics. One of the conventional metrics is the peak signal-to-noise ratio (PSNR) calculated for the original (noisy) image as

$$MSE^n = \sum_{i=1}^I \sum_{j=1}^J \frac{(I_{ij}^n - I_{ij}^{true})^2}{IJ}, \quad (2)$$

$$PSNR^n = 10 \log_{10} \left( \frac{255^2}{MSE^n} \right), \quad (3)$$

where  $I, J$  define image dimensions and it is supposed that the image is represented as 8-bit data.

It is also useful to estimate the image quality by some metric that takes into account the human visual system (HVS) and peculiarities of image understanding based on its low-level features. These can be, e.g., the visual quality metrics PSNR–HVS–M (Ponomarenko et al., 2007) or FSIM (Zhang et al., 2011). In particular,

$$PSNR - HVS - M^n = 10 \log_{10} \left( \frac{255^2}{MSE - HVS - M^n} \right),$$

where  $MSE - HVS - M^n$  is calculated in a set of 8x8 pixel blocks considering different sensitivity of HVS to distortions in different spatial frequencies as well as the masking effect (Ponomarenko et al., 2007).

Feature-SIMilarity (FSIM) is designed for grayscale images (or the luminance components of color images) and it represents the HVS-based metrics as well (Zhang et al., 2011). The underlying principle of FSIM is that HVS perceives an image mainly based on its salient low-level features. Specifically, two kinds of features, phase congruency (PC) and gradient magnitude, are used in FSIM, and they take into account complementary aspects of the image’s visual quality. The PC value is employed to weigh the contribution of each point to the overall similarity of the two images.

### 2.2. Used coder and filter

In our study, we use the BPG encoder that aims to replace the old JPEG format due to considerably better performance in the sense of higher quality and/or lower size of compressed data. This encoder has established itself as the one able to deal with most chroma formats (grayscale, YCbCr 4:2:0, 4:2:2, 4:4:4) and it has also proved to have OOP in the case of lossy compression for each of these formats (Kovalenko et al., 2022). These facts make this encoder extremely suitable for our purposes. Also note that the BPG encoder is simple to use – it has compression controlling parameter (CCP)  $Q$ , used internally to control the compression ratio and image quality.  $Q$  can vary in the range of 1 to 51 (Bellard et al., 2018) where larger  $Q$  results in a higher CR and corresponds to lower visual quality (in the case of compressing the noise-free images).

As was also mentioned, this paper focuses on the DCT-based filter that has been chosen based on several reasons. First, the DCT-based filters possess efficiency close to the best existing filters according to PSNR (Lukin et al., 2011). Second, they are characterized by efficient noise suppression in homogeneous image regions, excellent texture preservation, and good preservation of edges and details. Third, they can be easily adapted to signal-dependent and spatially correlated noise (Fevrlev et al., 2011). Fourth, filter properties can be easily controlled and varied by a single parameter  $\beta$  used in threshold setting.

To get a better understanding of these properties, let us briefly remind the basic principles of DCT-based

filtering. Denoising can be carried out in non-overlapping or overlapping blocks of, generally, arbitrary size and shape (Foi et al., 2007). Below, for simplicity and for providing high computational efficiency, we consider only the case of fixed 8x8 blocks. Direct DCT is carried out in each block. Then, a thresholding operation is applied to DCT coefficients except for the DC ones. Inverse DCT is then performed in blocks. Soft, hard, and combined thresholding can be used. Here, we apply hard thresholding and full overlapping of blocks. For optimal denoising according to PSNR,  $\beta$  should be about 2.7 whilst for providing the optimal visual quality it has to be slightly smaller, about 2.4 (Ponomarenko et al, 2011).

### 2.3. Fundamentals of lossy compression in OOP

Because this study aims to analyze the potential of post-filtering the noisy images that have been compressed in a lossy manner, it is reasonable to remind the main peculiarities of this type of compression. It has been already mentioned that, due to lossy compression, it is possible to reach an optimal operational point (if it exists), the ways to do this were described in our previous work (Kovalenko et al., 2022). To illustrate the phenomenon of OOP, the following method can be applied: in simulations, when one has a noise-free image, he/she adds AWGN to it, and applies lossy compression. Then, it is possible to calculate metrics for the whole range of Q values between a compressed image and the corresponding noise-free one. Examples of such dependencies on Q for six test images are presented in Fig. 2. OOP exists for five out of six images according to PSNR and only for one image according to the metric PSNR–HVS–M. There are cases when the metric steadily becomes worse (reduces) if Q increases. Then, OOP does not exist and it is necessary to understand what happens with compressed image post-filtering in such situations.

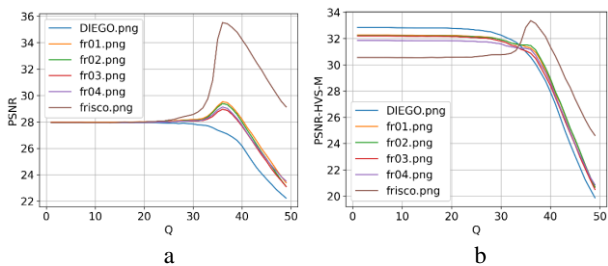


Fig. 2. Dependencies PSNR(Q) (a) and PSNR–HVS–M (Q) (b) for noise variance equal to 100

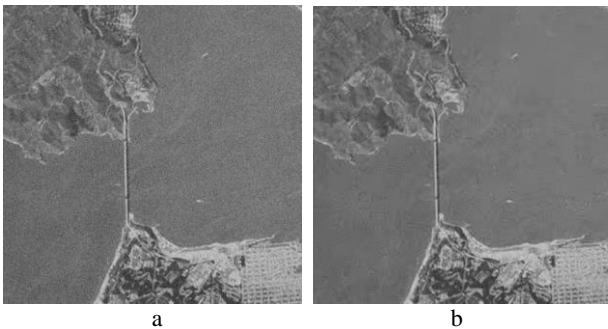


Fig. 3. Comparison between noisy (a) image and the image compressed in OOP (b)

The difference in quality can be noticed by comparing the noisy image and the one compressed in OOP placed side by side in Fig. 3. The filtering effect, which was mentioned earlier, is clearly visible, especially in homogeneous regions of the image. From Fig. 2, it can be seen that the improvement in quality is observed not only directly in the OOP, but also in its neighborhood.

### 3. Results of post-filtering after lossy compression in OOP and its neighborhood

#### 3.1. Assessment using the PSNR metric

The noise-free image was corrupted by the noise with a variance equal to 100, which is a good starting point for further research; after this, the noisy image was compressed by the BPG coder with Q in the limits from 24 to 35 (Q can be only an integer, Q = 24 corresponds to the case when the distortions due to lossy compression are invisible). After decompression, each of the obtained images was filtered by the DCT-filter with several values of  $\beta$ . Thus, let us analyze the compressed image quality after filtering using the PSNR metric. The obtained dependencies are presented in Fig. 4 for three values of Q.

Recall here that Q = 24 corresponds to visually lossless compression, Q = 30 relates to slightly visible distortions and Q = 35 is the (possible) OOP (see the plots in Fig. 2). Let us start our analysis with the Frisco image. From the obtained curves, it can be seen that there is a clear increase in quality for Q equal to 24 (Fig. 4, a, PSNR after just compression was about 28 dB, Fig. 2, a). The maximum PSNR (37.4 dB) for this case is at  $\beta = 2.8$ , after which the overall image quality starts to decrease monotonically, but it is still better compared to compressed but not post-filtered one. The next case is Q = 30 (Fig. 4, c) that is a little closer to OOP (although PSNR after compression is still about 28 dB, Fig. 2, a). The overall situation is still the same except for slightly smaller values of optimal  $\beta$  and the value of PSNR for it. The most interesting situation deals with post-filtering after compression in OOP (Fig. 4, e) where the compressed image quality (PSNR is about 35.5 dB) is already increased compared to the noisy one. Even in this case, the post-filtering can offer the quality increase with maximum PSNR = 36.7 dB for  $\beta = 2$ . But it is important to note that further increasing of  $\beta$  can lead to decreasing the overall image quality compared to the non-filtered one. In other words,  $\beta = 2$  allows to avoid oversmoothing. The reason for decreasing optimal  $\beta$  for larger Q can be explained in another way. In fact, the post-filter has to remove the residual noise having the variance that is smaller than the variance of the original noise. Then, a smaller threshold is needed for the DCT-based filter, and this is achieved by setting a smaller  $\beta$ .

Mainly, the same tendencies are valid for the fr03 image. Note that, for this image, the OOP according to PSNR is much less obvious (PSNR is about 28.7 dB, Fig. 2, a). The improvement due to post-filtering is observed for all three values of Q (Figures 4, b, 4, d, 4, f). For lossy compression with Q equal to 24 and 30 (Fig. 4, b, 4, d), obvious increase in PSNR for both cases is observed, but maxima take place for smaller optimal  $\beta$

values compared to the Frisco image in the same situation. Post-filtering after compression in OOP (Fig. 4, f) has the same properties as for Frisco (improvement of PSNR by 1.5 dB takes place).

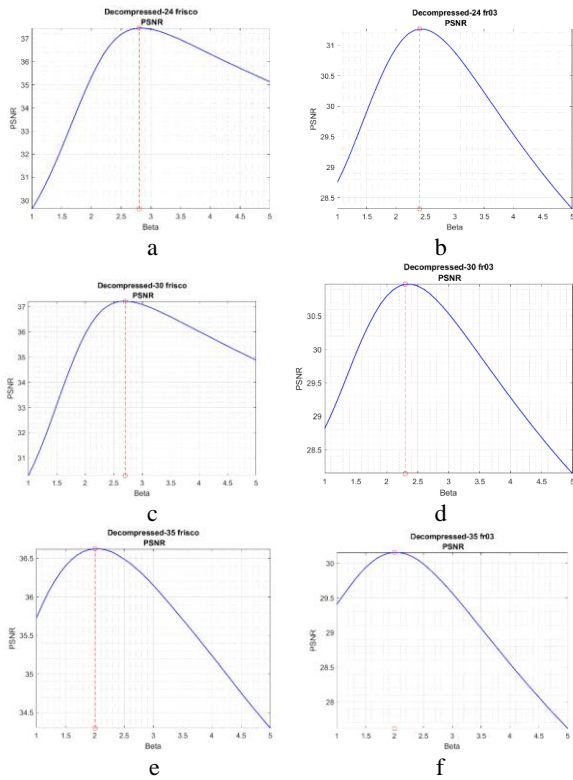


**Fig. 4.** Dependencies of PSNR calculated between the filtered and true images for noise variance equal to 100 for  $Q = 24$  (a, b),  $Q = 30$  (c, d),  $Q = 35$  (e, f)

**3.2. Assessment using the HVS-based metrics**

Let us also use the HVS-based metrics that can better represent real image quality. The obtained dependencies for the same images are presented in Figures 5 and 6.

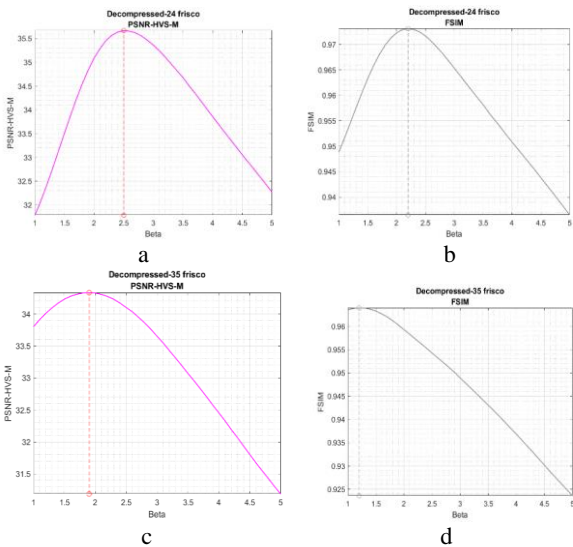


**Fig. 5.** Dependencies of PSNR–HVS–M:  $Q = 24$  (a),  $Q = 35$  (c) and FSIM:  $Q = 24$  (b),  $Q = 35$  (d) calculated between the post-filtered and true images Frisco for noise variance equal to 100

Firstly, let us analyze the dependencies for the image Frisco (Fig. 5). As one can see, the results are similar to the PSNR metric. We observe a sufficient increase of the metric values due to post-filtering for both  $Q < Q_{OOP}$  (see data in Fig. 5, a) and  $Q = Q_{OOP}$  (Fig. 5, c). Under condition of setting the optimal  $\beta$ , the improvement of PSNR–HVS–M is the latter case exceeds 1 dB and it can be easily noticed by visual inspection. Again, optimal  $\beta$  decreases if  $Q$  becomes larger.

The analysis for the FSIM metric confirms that image quality improves due to post-filtering. For  $Q = 24$ , FSIM = 0,937 after compression and 0,974 after post-filtering; for  $Q = 35$ , FSIM = 0,958 after compression and 0,964 after post-filtering. Keeping in mind the nonlinearity of this metric, these are significant improvements.

Analysis of results for the fr03 image (Fig. 6) shows similar tendencies – improvement is observed for both test images compressed with different  $Q$  for both PSNR–HVS–M and FSIM metrics (after compression with  $Q = 24$ , FSIM = 0,972; for  $Q = 35$ , FSIM = 0,97).

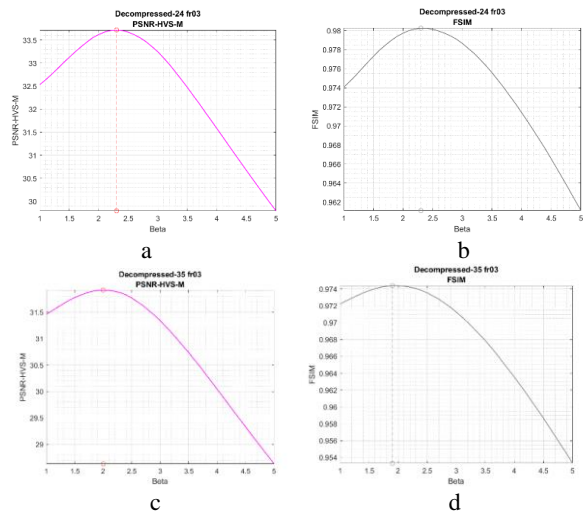


**Fig. 6.** Dependencies of PSNR–HVS–M (a, c) and FSIM (b, d) calculated between the post-filtered and true images fr03 for noise variance equal to 100

Summarizing the obtained results, the following intermediate conclusion can be drawn: post-filtering of lossy compressed noisy images seems reasonable since the improvement in quality can be obtained not only for relatively small values of  $Q$  (that are associated with rather small compression ratios) but also for  $Q$  values corresponding to OOP and its neighborhood. But here it is worth noting that with approaching  $Q$  for OOP, the optimal value of  $\beta$  parameter of the DCT filter is shifted to smaller values. As the result, it is recommended to use  $\beta$  from 1.5 to 2.5 depending on CCP used for lossy compression.

**3.3. Combined dependencies of HVS-based metric and visual analysis**

The next step is verifying the main observations using other values of noise variance. This time, we consider noise variance equal to 200. The obtained dependencies are presented in Fig. 7.

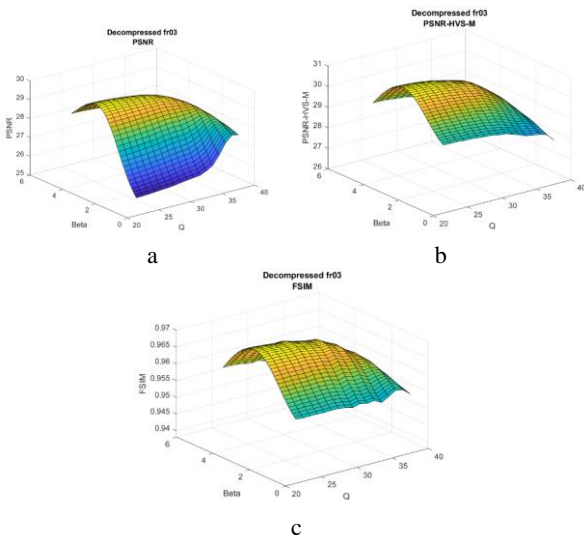


**Fig. 7.** 2D dependencies of PSNR (a), PSNR–HVS–M (b) and FSIM (c) on Q and  $\beta$

This time the obtained curves were represented as functions of two parameters to get surfaces (dependencies of metrics on two parameters). All three metrics have the same behavior: there is optimal  $\beta$  that decreases if Q increases; besides, the maximum value of the metric decreases if Q increases. This decrease is not too rapid. One also needs to admit that for the PSNR metric the peak (or maximum) is more obvious.

Let us give some examples of the results of our post-filtering approach. Fig. 8, a presents the noise-free test image Frisco, Fig. 8, b shows the same image corrupted by AWGN with a variance equal to 100. Noise is clearly seen, especially in homogeneous image regions. Thus, the image was compressed with  $Q = 27$  (Fig. 8, c) and filtered with  $\beta = 2.3$  (Fig. 8, d).

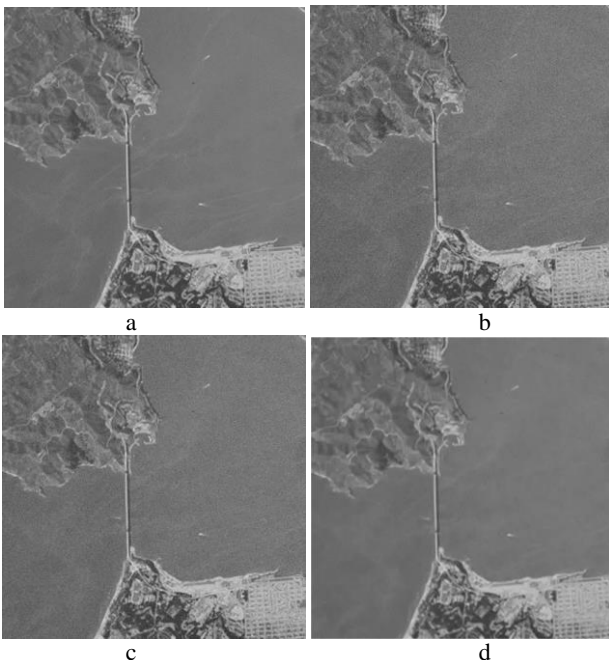


**Fig. 8.** Comparison of noise-free image (a), noisy with variance equal to 100 (b), compressed image with  $Q = 27$ , and filtered by DCT filter with  $\beta = 2.3$

From Fig. 8, c–d it is seen that noise is sufficiently suppressed whilst the useful information (edges,

textures, small-sized objects) is well preserved. That makes this post-filtering approach helpful for applications that require not only a large compression ratio but also better image quality compared to the usual lossy compression of noisy images.

#### 4. Conclusions and future work

The task of post-filtering lossy compressed images corrupted by AWGN is considered. The post-filtering brings specific features. It has been shown that the positive impact of post-filtering according not only to standard criteria such as PSNR but also according to HVS-based metrics such as PSNR–HVS–M and FSIM is observed. This increase is quite large and it exceeds 1 dB for PSNR and PSNR–HVS–M metrics for  $Q = Q_{OOP}$  and can be up to 7–9 dB for  $Q = 24$ , i.e. if visually lossless compression is performed. In  $Q = 24$  or slightly larger, then optimal  $\beta$  is about 2.3–2.5, if compression is done with  $Q$  about  $Q_{OOP}$ , then optimal  $\beta$  should be about 2.

In the future, it seems reasonable to test this approach for more images and try to implement this approach to multichannel images. Moreover, it seems possible to predict which filter value to use to get the best results in terms of image quality.

#### References

- Bazi, Y., Cavallaro, G., Demir, B., Melgani, F. (2022). Learning from Data for Remote Sensing Image Analysis. *International Journal of Remote Sensing*, 43(15-16), 5527–5533. DOI: 10.1080/01431161.2022.2131481.
- Bellard, F. (2018). BPG Image format. Retrieved from: <https://bellard.org/bpg/>.
- Blanes, I., Magli, E., Serra-Sagrista, J. (2014) A Tutorial on Image Compression for Optical Space Imaging Systems. *IEEE Geoscience and Remote Sensing Magazine*, 2(3), 8–26. DOI: 10.1109/MGRS.2014.2352465.
- Chatterjee, P., Milanfar, P. (2010). Is Denoising Dead? *IEEE Transactions on Image Processing*, 19(4), 895–911. DOI: 10.1109/TIP.2009.2037087.
- Christophe, E. (2011). Hyperspectral Data Compression Tradeoff. Prasad, S. et al. (eds). *Optical Remote Sensing. Augmented Vision and Reality*, 3. DOI: 10.1007/978-3-642-14212-3\_2.
- Colom, M., Buades, A., Morel, J.-M. (2014). Nonparametric noise estimation method for raw images. *J. Opt. Soc. Am.*, 31(4), 863–871. DOI: 10.1364/JOSAA.31.000863.
- Fevrale, D., Lukin, V., Ponomarenko, N., Abramov, S., Egiazarian, K., Astola, J. (2011) Efficiency analysis of DCT-based filters for color image database. *SPIE Conference Image Processing: Algorithms and Systems VII*, 7870.
- Foi, A. (2007). *Pointwise Shape-Adaptive DCT Image Filtering and Signal-Dependent Noise Estimation*: Thesis for the degree of Doctor of Technology. Tampere University of Technology, Tampere, Finland, 194.
- Hussain, A. J., Al-Fayadh, A., Radi, N. (2018). Image compression techniques: A survey in lossless and lossy algorithms. *Neurocomputing*, 300, 44–69.
- Kovalenko, B., Lukin, V. (2022). Usage of different Chroma Subsampling Modes in Image Compression by BPG Coder. *Ukrainian Journal of Remote Sensing*, 9(3), 11–16. DOI: 10.36023/ujrs.2022.9.3.216.
- Kovalenko, B., Lukin, V., Kryvenko, S., Naumenko, V., Vozel, B. (2022). BPG-Based Automatic Lossy Compression of Noisy Images with the Prediction of an

- Optimal Operation Existence and Its Parameters. *Applied Sciences*, 12(15), 7555. DOI: 10.3390/app12157555.
- Kovalenko, B., Lukin, V., Naumenko, V., Krivenko, S. (2021). Analysis of noisy image lossy compression by BPG using visual quality metrics. *IEEE 3rd International Conference on Advanced Trends in Information Theory (ATIT)*, 20–25.
- Lukin, V., Abramov, S., Ponomarenko, N., Egiazarian, K., Astola, J. (2011). Image Filtering: Potential Efficiency and Current Problems. *Proceedings of ICASSP*, 4.
- Ma, Y., Wu, H., Wang, L., Huang, B., Ranjan, R., Zomaya, A. & Jie, W. (2015). Remote sensing big data computing: Challenges and opportunities. *Future Generation Computer Systems*, 51, 47–60. DOI: 10.1016/j.future.2014.10.029.
- Mehmood, M., Shahzad, A., Zafar, B., Shabbir, A., Ali, N. (2022). Remote Sensing Image Classification: A Comprehensive Review and Applications. *Mathematical Problems in Engineering*, 2022(5880959), 24. DOI: 10.1155/2022/5880959
- Penna, B., Tillo, T., Magli, E., Olmo, G. (2007). Transform coding techniques for lossy hyperspectral data compression. *IEEE Transactions on Geoscience Remote Sensing*, 45(5), 1408–1421. DOI: 10.1109/TGRS.2007.894565.
- Ponomarenko, N., Lukin, V., Egiazarian, K. (2011). HVS-metric-based performance analysis of image denoising algorithms. *3rd European Workshop on Visual Information Processing*, 156–161. DOI: 10.1109/EuVIP.2011.6045554.
- Ponomarenko, N., Lukin, V., Zriakhov, M., Egiazarian, K. (2005). Lossy compression of images with additive noise. *Proceedings of International Conference on Advanced Concepts for Intelligent Vision Systems*, 3708(2005), 381–386.
- Ponomarenko, N., Silvestri, F., Egiazarian, K., Carli, M., Astola, J., Lukin, V. (2007). On Between-Coefficient Contrast Masking of DCT Basis Functions. *In Proceedings of the Third International Workshop on Video Processing and Quality Metrics for Consumer Electronics*, 4.
- Schowengerdt, R. A. (2007). *Remote Sensing: Models and Methods for Image Processing*. 3rd ed.; Academic Press: San Diego, CA, USA.
- Selva, E., Kountouris, A., Louet, Y. (2021). K-Means Based Blind Noise Variance Estimation. *2021 IEEE 93rd Vehicular Technology Conference (VTC2021-Spring)*, 1–7. DOI: 10.1109/VTC2021-Spring51267.2021.9449072.
- Simmer, K. U., Bitzer, J., Marro, C. (2001). Post-Filtering Techniques. In: Brandstein, M., Ward, D. (eds) *Microphone Arrays. Digital Signal Processing*. DOI: 10.1007/978-3-662-04619-7\_3.
- Zhang, L., Zhang, L., Mou, X., Zhang, D. (2011). FSIM: A Feature Similarity Index for Image Quality Assessment. *IEEE Transactions on Image Processing*, 20(8), 2378–2386. DOI: 10.1109/TIP.2011.2109730.

#### АНАЛІЗ ПОТЕНЦІЙНОЇ ЕФЕКТИВНОСТІ ПОСТ-ФІЛЬТРАЦІЇ ЗОБРАЖЕНЬ, УРАЖЕНИХ ШУМОМ, ПІСЛЯ СТИСНЕННЯ З ВТРАТАМИ

Б. В. Коваленко, В. С. Ребров, В. В. Лукін

Кафедра інформаційно-комунікаційних технологій ім. О. О. Зеленського, Національний аерокосмічний університет, 61070 Харків, Україна

Збільшення кількості зображень та їх розмірів є загальною тенденцією на сьогодні, але це веде до певних проблем із зберіганням і передачею такої кількості даних. Поширеним способом розв’язання цієї проблеми є використання стиснення з втратами, яке має не тільки більший коефіцієнт стиснення порівняно з підходами без втрат, але також має декілька особливостей. По-перше, спостерігається специфічний ефект фільтрації шуму. По-друге, може існувати оптимальна робоча точка (ОРТ), де якість стисненого зображення ближче до відповідного зображення без шумів згідно з вибраним показником якості. У цьому випадку варто стиснути це зображення в області ОРТ. Ці особливості були раніше вивчені і показали позитивні результати підвищення якості зображення. Але варто перевірити, чи можна додатково покращити якість шляхом використання пост-фільтрації. У цьому дослідженні ми намагаємося відповісти на запитання: “чи варто фільтрувати зображення після стиснення з втратами, особливо в околі ОРТ? Яку користь це може принести в сенсі якості зображення?”. Дослідження проводиться для BPG-кодеру та фільтру на основі ДКП для адитивного білого шуму, зосередившись головним чином на однокомпонентних зображеннях у градаціях сірого. Якість зображення оцінюється кількома показниками, такими як PSNR, PSNR–HVS–M і FSIM. Продемонстровано можливе підвищення якості зображення за допомогою пост-фільтрації та надано рекомендації щодо кращого параметра фільтру.

**Ключові слова:** зображення у градаціях сірого, стиснення зображень із втратами, оптимальна робоча точка, кодер BPG, пост-фільтрація, фільтр на основі ДКП.

Рукопис статті отримано 16.02.2023